

Article

The Study of the Mechanism of Protein Crystallization in Space by Using Microchannel to Simulate Microgravity Environment

Yong Yu ^{1,*}, Kai Li ^{1,2,*}, Hai Lin ¹ and Ji-Cheng Li ^{1,2}

¹ CAS Key Laboratory of Microgravity, Institute of Mechanics, Chinese Academy of Sciences, Beijing 100190, China; cas5@imech.ac.cn (H.L.); lijicheng@imech.ac.cn (J.-C.L.)

² School of Engineering Sciences, University of Chinese Academy of Sciences, Beijing 100049, China

* Correspondence: yuyong@imech.ac.cn (Y.Y.); likai@imech.ac.cn (K.L.)

Received: 23 August 2018; Accepted: 21 October 2018; Published: 24 October 2018



Abstract: Space is expected to be a convection-free, quiescent environment for the production of large-size and high-quality protein crystals. However, the mechanisms by which the diffusion environment in space improves the quality of the protein crystals are not fully understood. The interior of a microfluidic device can be used to simulate a microgravity environment to investigate the protein crystallization mechanism that occurs in space. In the present study, lysozyme crystals were grown in a prototype microchannel device with a height of 50 μm in a glass-polydimethylsiloxane (PDMS)-glass sandwich structure. Comparative experiments were also conducted in a sample pool with a height of 2 mm under the same growth conditions. We compared the crystal morphologies and growth rates of the grown crystals in the two sample pools. The experimental results showed that at very low initial supersaturation, the morphology and growth rates of lysozyme crystals under the simulated microgravity conditions is similar to that on Earth. With increasing initial supersaturation, a convection-free, quiescent environment is better for lysozyme crystal growth. When the initial supersaturation exceeded a threshold, the growth of the lysozyme crystal surface under the simulated microgravity conditions never completely transform from isotropic to anisotropic. The experimental results showed that the convection may have a dual effect on the crystal morphology. Convection can increase the roughness of the crystal surface and promote the transformation of the crystal form from circular to tetragonal during the crystallization process.

Keywords: protein crystallization; simulated microgravity; microchannel

1. Introduction

The high-quality protein crystals are crucial for the determination of protein structures using X-ray diffraction (XRD). The process of protein crystallization produces a solute concentration gradient that leads to buoyancy drive convection [1]. Convection could change the local degree of supersaturation and the impurity concentration at different locations on the crystal surface [2].

There is a popular belief that diffusion-controlled transport can improve the quality of protein crystals [3]. Sedimentation movement and convective flow due to gravity are negligible under microgravity conditions [4,5]. Therefore, Space is thought to be a quiescent environment for the production of large enough size and high-quality protein crystals. A series of experiments in space have been conducted to grow protein crystals [3,6–16], and an analysis of the X-ray quality of the crystals grown in space was performed [17]. The experimental results showed that protein crystals of high diffraction quality could be obtained [3,10]. Unfortunately, some research showed that only

about 20% of the protein crystals grown in the space environment exhibited higher quality than the corresponding terrestrial cases [18,19]. For reasons that the rate of improvement is low, one view is that this was attributed to the unreliability of space shuttle flights, the short duration of space shuttle flights, the potentially harmful gravitational forces experienced on re-entry, instability of temperature control during sample transfer operations, and other logistical difficulties [10]. There is some truth to this view, such as it has often been difficult to separate the effects of microgravity from the effects of the flight hardware, and the relative contributions of the microgravity environment and the hardware for a particular experiment have often been unclear [20]. Using the Advanced Protein Crystallization Facility, Vergara et al. [21] had compared the crystallographic quality of protein crystals grown in microgravity with that grown in parallel on earth gravity under otherwise identical conditions. The statistical analysis revealed that about half of the crystals produced under microgravity had a superior X-ray diffraction limit in respect to the terrestrial controls. The rate of improvement of the crystal quality is not too bad from the homogeneous data derived for a single facility. Recently, some studies suggested that the main reason is that no one has fully clarified the mechanisms by which microgravity improves the quality of many protein crystals [18,22,23]. If this problem can be understood, it will greatly promote the utilization of microgravity resources. In view of the complexity of protein crystallization, the research on this issue will face great challenges, which is also the interest of the research on this issue.

In fact, research has been going on about how the space environment can improve the quality of protein crystals. Judge et al. [24] had compiled many data and results of the macromolecular crystallization experiments flown in microgravity, hoping to identify factors that result in success and those that result in failure. But they cannot identify any predictive technique to establish if a crystallization experiment will benefit from microgravity. At present, the most popular explanation for the quality improvement of protein crystals grown in the space environment is related to the impact of impurities on protein crystallization [18,25–32]. Impurities are considered harmful to protein crystallization. In the space environment, the slow diffusion rate can reduce the impurity transmission to the crystal surface. Therefore, the effect of impurities on protein crystallization is the main research direction [26–28,30,32,33]. Research does confirm this effect of microgravity on impurities such as the hen egg white lysozyme dimer partitioning in protein crystal growth [32]. However, in another experiment a space protein crystallized using an egg white lysozyme (CEWL), which contained various natural lysozyme dimer impurities [33]. The experiment results showed no significant favorable differences in impurity incorporation between microgravity and ground crystal samples were observed. At a low impurity concentration the microgravity crystals preferentially incorporated the dimer. The effect of microgravity aiding in the partitioning of the impurity is complex, which can be so different under different conditions and vary from system to system [33]. In addition, this theory also only holds for the impurities of larger molecular weight than the crystal growth units, and the contradictory conclusion will be drawn when it comes to the impurities of smaller molecular weight [22]. Protein crystallization is a complicated process involving many factors, and the effect of impurities may be only a part of the influence of the space environment on protein crystallization.

Studying the effect of microgravity on the growth mechanism of protein crystals may solve this problem. At present, space experiments have begun to study the growth mechanism of protein crystals in a space environment [18,23]. The seed crystal has to be used to measure the growth rate under microgravity [23]. The best way to analyze the mechanism of protein crystal growth is by combining the info of growth, including the growth rate and morphology, and the transport processes. Very accurate diffusion data on the lysozyme-NaCl system is available [34]. Protein crystals are likely to grow in a random location in the sample pool, and the initially grown protein crystals are very small. The study of the mechanism of protein crystallization requires the development of special space experimental facilities to automatically search for newly growing crystals and focus on the crystal surface, measuring the transport processes. The interferometric analysis for measuring transport processes has been provided in some space experiments using the Protein Crystal Diagnostic

Facility [35]. However, the direct experimental study in space is limited by restricted access and high costs. The best strategy is to conduct Earth-based pre-research on the protein crystallization mechanism under simulated microgravity conditions, and then further validate the theory through space experimentation. To this purpose, the magnetic field [36–38] and gel methods [39] have been used to reduce the effect of convective flow on protein crystallization. However, one drawback to the magnetic field method is that the magnetic field can influence the orientation and the growth of the protein crystals [37]. In addition, the magnetic force pushes the protein crystals to locations where the magnetic field is strongest, and the crystals are likely to pile up and form twin crystals. As for the gel method, the addition of gel and other high viscosity medium in a solution can inhibit the flow of the solution, but the mixing of these macromolecules has a great influence on nucleation. Van Driesche et al. described that gel itself acts as a complex impurity, and crystal growth in a gelled solution is not an ideal convection-free process [40].

With the development of MEMS (Micro-Electro-Mechanical System) technology, microfluidics is currently one of the most rapidly growing frontier fields. Using this technique, the transport phenomena can be effectively controlled since there are no buoyancy-driven convection instabilities on such a small scale [41–44]. From the viewpoint of fluid mechanics, microfluidics offers the unequalled ability to provide a simulated microgravity environment on Earth. However, protein crystal growth in a microchannel has some different aspects compared with space due to the small dimensions of the microchannels. In fact, the protein crystals that grow inside the microchannel are not suspended in the solution, and they still sink to the bottom of the microchannel by gravity. However, the convective flow can be inhibited significantly due to the small size of the microchannels, and the mass transfer process is diffusion controlled in the process of protein crystal growth. Although the confined geometries may influence the full growth of the crystal facet and the microchannel surface may influence the crystallization nucleation [45], the microchannel can be used to study the growth of the protein crystal after nucleation. The use of microchannels is the same as the use of capillaries placed perpendicular to the direction of gravity to obtain protein crystals in a confined volume. The latter is a historically well-known concept and a practical technique [46], however, microchannels are more suitable for studying the crystallization mechanism. In addition, due to shuttles or the International Space Station (ISS) movements, there are g-jitters that induce crystal movements in real microgravity environments [47]. The microchannel cannot reproduce this effect, which is always present in microgravity experiments.

Microfluidics-based protein crystallization devices have been developed as an excellent and cost-effective apparatus for protein crystallization [48]. Microfluidic approaches are attractive for protein crystallization, because they (a) can carry out many experiments simultaneously to cover a dense, multidimensional chemical space; (b) use very small quantities of samples; (c) precisely control mixing, interfaces, and time of contact between solutions; and (d) the crystal quality can be evaluated by X-ray diffraction [49–57]. Some microfluidic devices for the high-throughput screening of protein crystallization conditions have been designed, including the free-interface diffusion [50,51], droplet-based [43,44,52–54], system based on the Slip Chip [42,43,48] and microdialysis-based methods [55,56]. A commercial off-the-shelf microfluidic device was tested in microgravity using a high-throughput protein crystal growth method [58]. However, there is no existing microfluidics-based research on the mechanism of protein crystallization in space.

In this paper, a prototype microchannel device was used for protein crystallization, which consists of a circular cavity made by a glass-PDMS-glass system with a height of 50 μm . The device reduces buoyancy-driven convection to simulate a microgravity environment for protein crystal growth. Lysozyme crystals were grown in a microchannel, and comparative experiments were conducted in a sample pool with a height of 2 mm in the same conditions. Our purpose is to investigate the mechanism of protein crystallization under microgravity conditions rather than the effect of impurities on protein crystal growth. The crystal morphologies and crystal growth rates of the grown crystals were compared and the differences were analyzed in detail. Note that at the high supersaturation

condition, the formation of a critical nucleus was easier in the bulk solution rather than on the wall surface [59]. Hence, lysozyme crystals were nucleated and grown using the isothermal batch method to reduce the influence of the microchannel surface on the crystallization nucleation. But the batch method induces a very fast crystallization, reducing the benefit of microgravity compared to free-interface diffusion, dialysis, or gel acupuncture methods [60].

2. Experiments

2.1. The Experiment Devices

The diffusion Grashof number, a dimensionless number, is used to describe the buoyancy convection produced in the process of crystal growth. Its physical meaning is the ratio of buoyancy to viscous force in inhomogeneous media. The smaller the Grashof number is, the smaller the buoyancy convection. The diffusion Grashof number is defined as

$$\text{Gr}_D = gL^3\beta_c\Delta C/\nu^2 \quad (1)$$

where g is the acceleration due to gravity, ν is the kinematic viscosity, β_c is the solution expansion coefficient, and ΔC is the concentration difference. L is the characteristic length; the height of the solution in the gravity direction can be used as the value of L .

A sample pool with the height of 2 mm and a glass-PDMS-glass microchannel with the height $L_M = 50 \mu\text{m}$ were used in the present study. For the sample pool on Earth, the characteristic length is $L_P = 2 \text{ mm}$, and the corresponding diffusion Grashof number Gr_D^P is

$$\text{Gr}_D^P = gL_P^3\beta_c\Delta C/\nu^2 \quad (2)$$

For the glass-PDMS-glass microchannel, with the characteristic length $L_M = 50 \mu\text{m}$, the corresponding diffusion Grashof number Gr_D^M is

$$\text{Gr}_D^M = 1.56 \times 10^{-5}\text{Gr}_D^P \quad (3)$$

The above calculation shows that the microchannel can effectively restrain buoyancy convection. If using the same ν , β_c and ΔC , the ability of suppressing the buoyancy convection using the microfluidic device with the height of $50 \mu\text{m}$ is comparable to that using the sample pool with the height of 2 mm in the microgravity environment ($1.56 \times 10^{-5} \text{ g}$).

As shown in Figure 1, the microfluidic device proposed in the present study is a glass-PDMS-glass sandwich structure. The depth of the microfluidic device is $50 \mu\text{m}$. Two circular cavities with different diameters were designed to investigate the effects of the solution volume on the crystal growth in the microchannel. However, it was found that the volume change of solution in the microchannel had no effect on the crystal morphology and the crystal growth rates. The microfluidic device was fabricated by multilayer soft lithography techniques using PDMS. A mixture of liquid prepolymer PDMS and its cross-link agent at a quality ratio of 10:1 was poured onto a mold and cured at 353 K for two hours. The solidified PDMS structures were then peeled off, and small holes were drilled into the PDMS layer to produce an inlet and outlet at the position shown in Figure 1. The surface of the PDMS layer with microchannel and a glass slide were exposed to oxygen plasma for about four minutes and then the two exposed surfaces pressed against each other. The ensemble was heated again to 353 K for half an hour, which led to the formation of an irreversible PDMS-glass system. In the same way, another glass slide with two holes and the PDMS-glass system were impacted together to form the glass-PDMS-glass sandwich structure. Pipes were inserted into the inlets and outlets. Because PDMS is permeable to gas, an epoxy resin was used to wrap the exposed areas of PDMS. The areas surrounding the inlets and outlets were sealed with silicone rubber and then coated with epoxy resin.

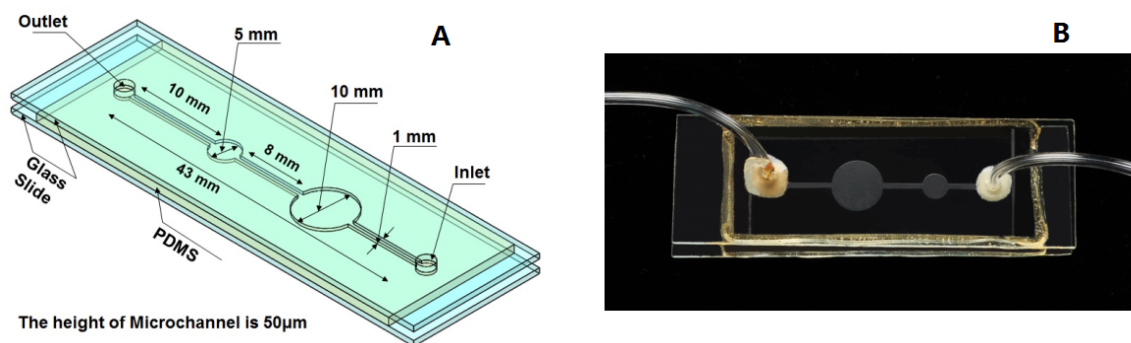


Figure 1. Schematic and photography of the microfluidic device. (A) Schematic of the microfluidic device; (B) photography of the microfluidic device.

2.2. Reagents and Methods

An HAC-NaAc buffer solution (250 mM, pH 4.50) was used, and chicken egg-white lysozyme was purchased from Sigma (St. Louis, MO, USA). High-purity deionized water (18.2 M Ω) was obtained by passing distilled water through a Milli-Q (Millipore Company, Billerica, MA, USA) Plus water purification system, and all other reagents were of an analytical grade.

The buffer solution was filtrated with a 0.22 μm filtration membrane before performing the experiments, and appropriate amounts of lysozyme powder and NaCl were then dissolved separately in a buffer solution. These solutions were kept at 277 K. The lysozyme solution was centrifuged at 14,000 $\times g$ r/min for about thirty minutes, and then the upper half of the solution in a centrifuge tube was used in the experiments.

The lysozyme crystals were nucleated and grown using the isothermal batch method to reduce the influence of microchannel surface on the crystallization nucleation. The initial protein concentration C_{∞} , NaCl concentration C_s and the corresponding supersaturations $\sigma = (C_{\infty} - C_s)/C_s$ in experiments are shown in Table 1. The equilibrium saturation concentration of lysozyme C_s is 6.29 $\text{mg}\cdot\text{mL}^{-1}$ in 293 K and pH 4.50.

Table 1. The concentration of lysozyme crystal solutions (293 K \pm 0.5 K, pH 4.50).

	Lysozyme ($\text{mg}\cdot\text{mL}^{-1}$)	NaCl (M)	Supersaturation
1	13.3	1.00	1.11
2	16.7	1.00	1.65
3	20.0	1.00	2.18
4	26.7	1.00	3.24
5	33.3	1.00	4.29

The NaCl solution and clear lysozyme solution were well mixed and injected into the microfluidic device and the sample pool, and then the pipe orifices of the microchannel and the sample pool (as shown in Figure 1) were sealed at once. The microfluidic device and the sample pool were placed in a biochemical incubator. During the process, the ambient temperature and the temperature of the solutions were kept higher than the controlled temperature inside of the biochemical incubator to avoid too high supersaturation. Observations of the morphology and measurement of the growth rates of the lysozyme crystals were carried out using a microscope. The space group of the tetragonal lysozyme crystal is P4₃2₁2. Figure 2 shows the illustration of the normal growth habit of tetragonal lysozyme crystals [61] and an observed lysozyme crystal. The growth rates of the crystal were measured by selecting (110) face.

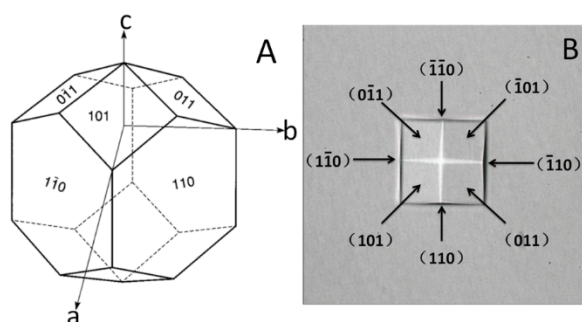


Figure 2. Illustration of the normal growth habit of tetragonal lysozyme crystals and a lysozyme crystal observed. (A) Illustration of the normal growth habit of tetragonal lysozyme crystals; (B) a lysozyme crystal observed.

3. Results and Discussion

3.1. The Morphologies of the Grown Lysozyme Crystals

Figure 3(a1–e1) show the morphologies of the crystals grown in the microfluidic device and in the sample pool with different initial supersaturations at a specific time after the mixing of the NaCl solution and clear lysozyme solution. Due to the limited height of 50 microns of the microchannel, the data of the crystals with the height less than 50 microns in the gravity direction (i.e., the direction normal to the photograph plane) are selected. Figure 3(a2–e2) show the corresponding morphology evolutions of the crystals grown in the microchannel and in the sample pool. It can be seen that at the low initial supersaturation $\sigma = 1.11$, the appearances of crystals were smooth and perfect in both the microfluidic device and the sample pool. At higher initial supersaturations, i.e., $\sigma = 1.65$ and 2.18 , the appearances of grown crystals in the microfluidic device remained smooth and perfect while the surfaces of those in the sample pool became increasingly rough as shown in Figure 3b,c. When the initial supersaturation increased to $\sigma = 3.24$, the surfaces of crystals grown in the microchannel also became rough while the morphologies of the crystals grown in the sample pool were even worse, and large caves and steps emerged on the crystal surfaces, as shown in Figure 3d. Note that when the crystal growth reached the height of the microchannel device, the top faces of the crystal fused into a plane; e.g., see the crystal morphologies at 24 h in Figure 3(a2).

As shown in Figure 3e, when the initial supersaturation further increased to $\sigma = 4.29$, the surfaces of crystals grown in both the microchannel and sample pool became very rough. Dendritic crystals emerged in both the microchannel and the sample pool. However, the crystals grown in the sample pool gradually evolved from the circular form to the tetragonal form throughout the crystallization process, while those in the microchannel did not completely transform from circular to tetragonal.

As the initial supersaturation level increased, the morphology of the crystals grown in the microchannel gradually changed. The morphology of the crystals grown in the microchannel were showed in Figure 4. Although the transport of macromolecules towards a growing crystal is isotropic, the interfacial incorporation process is anisotropic because the bond distribution in the crystal structure is anisotropic [25,62]. Therefore, the growth rate for every crystal face is different. At the initial supersaturation $\sigma = 4.29$, the morphology of the crystal grown in the microchannel did not completely transform from circular to tetragonal throughout the crystallization process, which implied the growth of every surface never completely transforms from isotropic to anisotropic. However, the single crystals should be anisotropic because the bond distribution in the single crystal structure is anisotropic.

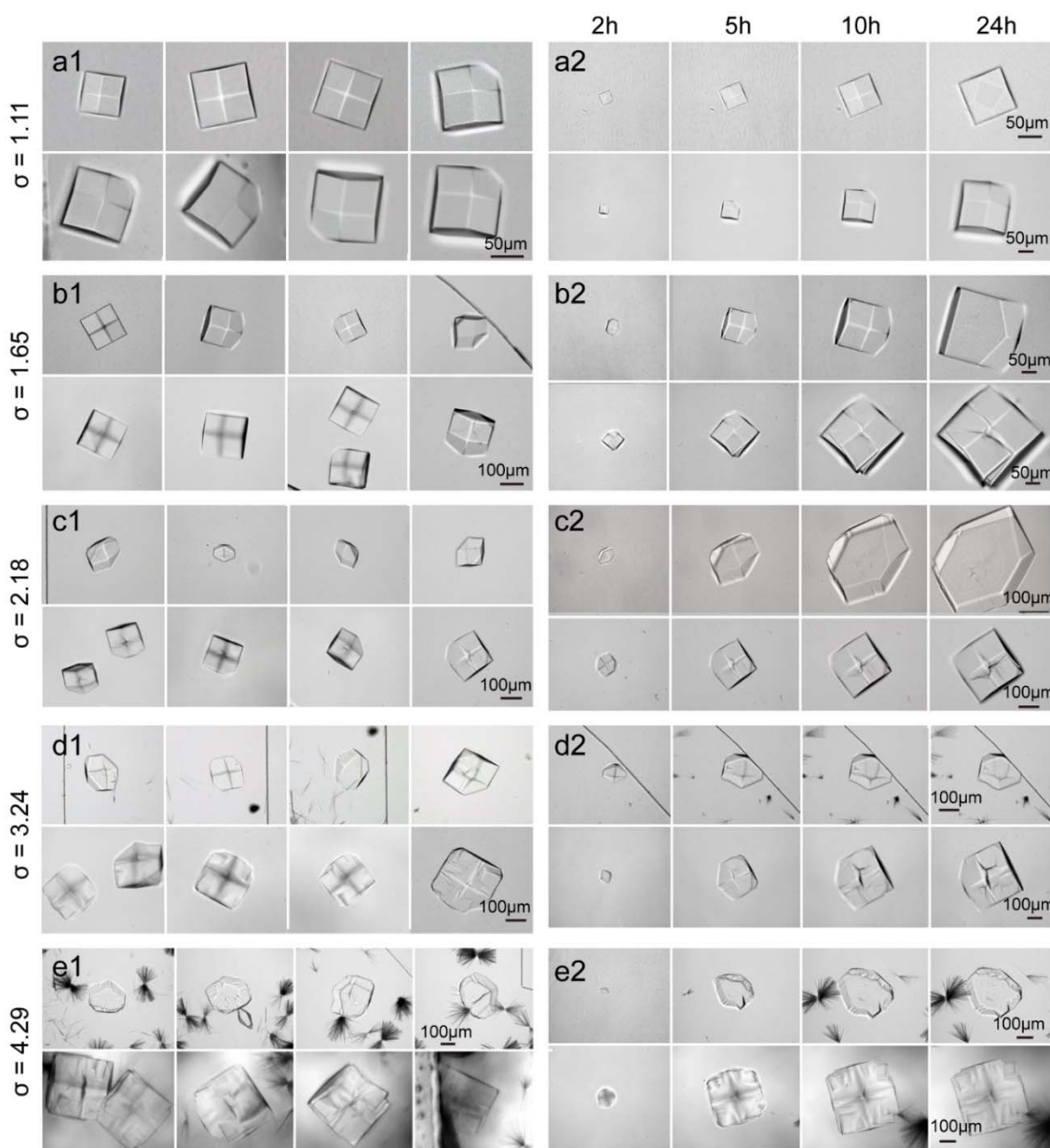


Figure 3. The morphologies of crystals grown in the microchannel and the sample pool. The experimental conditions are as shown in Table 1. In each set of experimental data, the morphologies of crystals grown in the microchannel were above and the morphologies of crystals grown in the sample pool were below. (a1–e1) shows the morphologies of the crystals grown in the microfluidic device and in the sample pool with different initial supersaturations at a specific time after the mixing of the NaCl solution and the clear lysozyme solution. The photo shoot time after the mixing of the NaCl solution and the clear lysozyme solution: (a1): 10 h; (b1): 10 h; (c1): 5 h; (d1): 5 h; (e1): 24 h. (a2–e2) shows the morphology evolutions of the crystals grown in the microfluidic device and in the sample pool.

The intensity of convection increases with the rise of supersaturation. The effect of convection on the protein growth mechanism may be manifold. Novel investigations suggest that the protein molecules can form oligomers already in the crystallization solution [63], rather than entering the crystal lattice one-by-one. Ferreira et al. [63] thought that the mesoscopic clusters are beneficial when they accelerate the formation of the first precrystalline nuclei and are detrimental as they deplete the solution of protein ready to crystallize. Nadarjah et al. [64] thought that the growth of a protein crystal was a two-step process: aggregate growth units are first formed in the bulk solution by stronger

intermolecular bonds and then attached to the crystal face by weaker bonds. Nadarjah et al. [64] figured that the growing unit for the (110) face may be octamer corresponding to 4_3 helix while the growing unit for the (101) face may be a tetramer corresponding to the 4_3 helix [61].

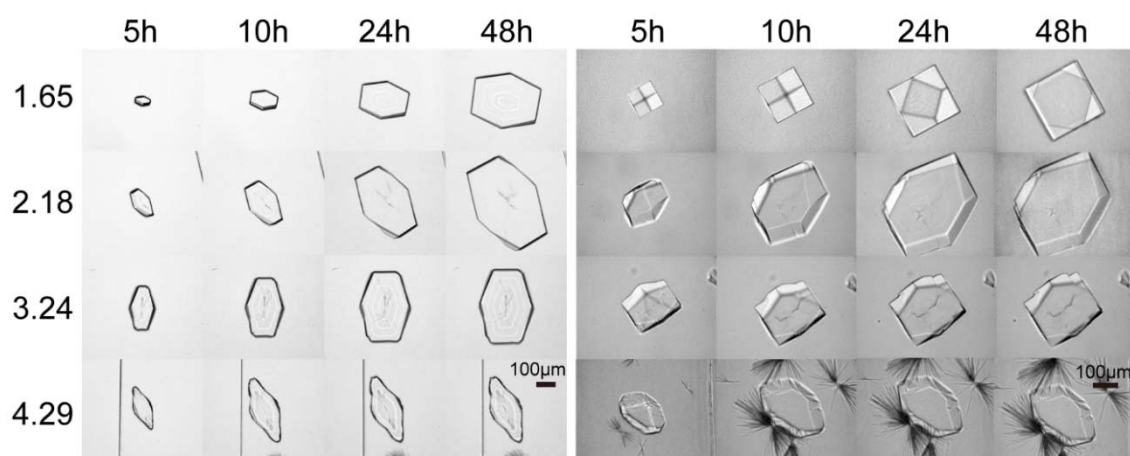


Figure 4. The morphology evolutions of the crystals grown in the microchannel with the increasing initial supersaturation.

Convection should have a great influence on the aggregate reactions. Convection can promote the collision of the protein molecules to form aggregates and transports more growth units to the surface of the crystal. Therefore, convection increases the roughness of the crystal surface. When the supersaturation is low, the influence may not be obvious. But as supersaturation rises, the trend will become more pronounced. When the supersaturation is high, the protein molecules readily form oligomers and dendritic crystals in the crystallization solution. Many mesoscopic clusters are connected by weak bonds. The high intensity convection can stir and break these mesoscopic clusters connected by weak bonds, making the aggregate in the solution more evenly distributed. Therefore, under the condition of higher supersaturation, convection should be favorable for protein crystallization.

Convection is also likely to have an effect on protein growth units on the crystal surface. When the protein growth units are transferred to a growing crystal and absorbed on the crystal surface, there are two ways for the growth units to enter the crystal lattice. One way is that the protein growth units remain attached to the crystal surface and are wrapped into the crystal structure with the crystal growth. The other way is that the protein molecules enter the crystal lattice by moving to the right position and rotating to the correct orientation, attaching to the interior of the lattice with the strongest bonds, which is time-consuming. At low supersaturation, few protein growth units are transferred to the crystal surface. Except for some of the molecules that desorbed and come back into the solution, most of them could enter the crystal lattice in the second way.

With increasing supersaturation, more protein growth units are transferred to the crystal surface. At high supersaturation, surface roughening occurs, so the growth units have two or three surfaces exposed to the crystal surface, resulting in a much higher link density. Many growth units may not be in the right direction or in the correct position to interact with the crystal surface. On the one hand, they need to overcome the larger energy barrier to enter the crystal lattice in the second way. On the other hand, they do not have enough time to do it because the new growth units are quickly transferred. In addition, the mesoscopic clusters near the crystal surface may be adsorbed on the crystal surface to affect the crystal quality.

The strength of the lattice defect interaction is diverse and weaker than the strongest bonds. If there are disturbances on the interface, such as convection, some protein growth units connected by the relatively weak interactions will be forced off from the interface and reintroduced into the surrounding solution while the growth units linked by the relatively stronger bonds inside the crystal structure will remain. Convection can also remove the mesoscopic clusters that are adsorbed on

the surface of the crystals. It is possible that the crystal quality will be improved. Previously Akio Kadowaki et al. was puzzled to find that the crystal quality grown under forced flow was better than that grown in quiescent conditions [65]. In that case convection is beneficial to the crystal growth.

In a word, the convection may have a dual effect on the crystal morphology. Convection can increase the roughness of the crystal surface and promote the transformation of crystal form from circular to tetragonal during the crystallization process.

3.2. The Growth Rates of the Lysozyme Crystals

After the mixing of the NaCl solution and clear lysozyme solution, the growth rates of the (110) face of the lysozyme crystals between 2 h and 5 h was measured. The growth rates of the crystal were measured by selecting (110) faces that are parallel to the gravity direction, to avoid the geometrical influence of the microchannel. The growth rates of the (110) face of five selected crystals were averaged and the uncertainty was given by the dispersion. Under the condition of supersaturation $\sigma = 4.29$, the growth rates of the crystal that can distinguish (110) surfaces were measured. The results were listed in Table 2 and plotted in Figure 5. The x-coordinate is the initial supersaturation, and the error bar is the standard deviation of uncertainty. It should be noted that the supersaturation at the crystal surface is different from the bulk supersaturation, particularly in non-convective environments. It can be seen that for lysozyme crystals grown in both the microchannel and sample pool, the growth rates of the (110) face increased with the initial supersaturation increase. At the initial supersaturation $\sigma = 1.11$, the growth rates of the (110) face were nearly the same for the crystals grown in the microchannel and the sample pool. Between $\sigma = 2.18$ and $\sigma = 3.24$, the growth rates of the (110) face for the crystals grown in the microchannel increased little with supersaturation.

During the Nanostep experiment of the Japan Aerospace Exploration Agency (JAXA), the crystal growth rates were determined by interferometry on board of the ISS [24]. Weichun Pan et al. also monitored the behaviors of crystal growth under various gravity conditions via the Foton Satellite and parabolic flight [18]. In the study, protein crystallization experiments under microgravity conditions were carried out. The effects of dimer molecules on step velocity and normal growth rate were investigated. They found the crystal growth rate in the microgravity environment is a little faster than that on Earth under certain conditions. In Foton satellite experiments [18], the experimental results show that when $C_{\text{NaCl}} = 2.1\%$, the crystal growth rate in the microgravity environment is a little faster than that on Earth with the supersaturation around 3.65, 3.80 and 3.9, respectively, while it was lower than that on Earth with the supersaturation around 3.70. When $C_{\text{NaCl}} = 2.5\%$, the crystal growth rate in the microgravity environment was faster than that on Earth only with the supersaturation around 4.0, while it was lower than that on Earth with the supersaturation around 3.5 and 4.5, respectively. The space experimental data presents a significant fluctuation, which may contribute to occasional unstable conditions such as unavoidable mechanic vibration during samples shipping and rocket launching [18]. Their results differ from those of the study, which may be due to the different amounts of precipitant. After all, the concentration of the precipitator can affect the growth rate of the crystals [33].

Table 2. The growth rates of the (110) face of lysozyme crystal.

σ	Growth Rates in the Microchannel (nm/s)	Growth Rates in the Sample Pool (nm/s)
1.11	1.21 ± 0.21	1.16 ± 0.06
1.65	2.48 ± 0.23	2.74 ± 0.06
2.18	3.18 ± 0.14	4.14 ± 0.21
3.24	3.36 ± 0.26	6.75 ± 0.93
4.29	7.35 ± 1.16	10.65 ± 0.63

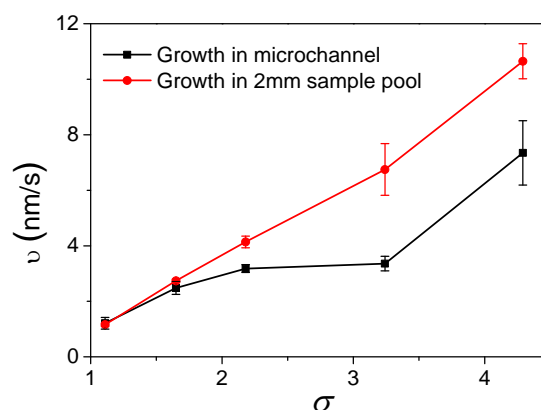


Figure 5. Comparison of the growth rates of the (110) face of the lysozyme crystals grown in the microchannel and the sample pool between 2 h and 5 h at different bulk supersaturations.

4. Conclusions

A microfluidic device was used to simulate a microgravity environment and investigate the resulting protein crystallization mechanisms. We used a sample pool with a height of 2 mm as a control, and compared the crystal morphologies and the growth rates of convectively and diffusively grown crystals. When the initial supersaturation was low, there were no significant differences in the morphologies and the growth rates of the lysozyme crystals in both environments. With the increasing convective transport of protein molecules due to the initial supersaturation increase, the surfaces of the lysozyme crystals grown in the convective environments were rougher. Moreover, when the initial supersaturation exceeded a certain threshold, the morphology of the crystals grown in the diffusive environment did not completely transform from circular to tetragonal throughout the crystallization process, indicating the growth of the surface never completely transformed from isotropic to anisotropic. The experimental results showed that the convection may have a dual effect on the crystal morphology. Convection can increase the roughness of the crystal surface, and promotes the transformation of the crystal form from circular to tetragonal during the crystallization process. In our future work, we will compare the quality of protein crystals grown in microchannels and sample pools.

It should be noted that protein crystal growth in the microchannel has some different aspects compared with that in space, such as the effects of the confined geometries and the larger surface-to-volume ratio, although in the present study lysozyme crystals were nucleated and grown using the isothermal batch method to reduce the influence of the microchannel surface on the crystallization nucleation. Therefore, further validations of the conclusions are required to be conducted through space experiments in the future.

Author Contributions: Conceptualization, methodology, formal analysis, investigation, data curation, writing—original, resources, Y.Y.; funding acquisition, writing—review, supervision, project administration, K.L.; visualization, H.L., draft preparation, writing—editing, J.-C.L.

Funding: This research is supported by the National Nature Science Foundation of China (No. 11472282 and 11672311).

Conflicts of Interest: The authors declare no conflict of interest. The funders had no role in the design of the study; in the collection, analyses, or interpretation of data; in the writing of the manuscript, or in the decision to publish the results.

References

1. Pusey, M.; Witherow, W.; Naumann, R. Preliminary investigations into solutal flow about growing tetragonal lysozyme crystals. *J. Cryst. Growth* **1988**, *90*, 105–111. [[CrossRef](#)]
2. Bennema, P. Crystal growth from solution—Theory and experiment. *J. Cryst. Growth* **1974**, *24*, 76–83. [[CrossRef](#)]

3. Caylor, C.L.; Dobrianov, I.; Lemay, S.G.; Kimmer, C.; Kriminski, S.; Finkelstein, K.D.; Zipfel, W.; Webb, W.W.; Thomas, B.R.; Chernov, A.A. Macromolecular impurities and disorder in protein crystals. *Proteins Struct. Funct. Bioinform.* **1999**, *36*, 270–281. [[CrossRef](#)]
4. Strellov, V.I.; Kuranova, I.P.; Zakharov, B.G.; Voloshin, A.E. Crystallization in space: Results and prospects. *Crystallogr. Rep.* **2014**, *59*, 781–806. [[CrossRef](#)]
5. McPherson, A. *Cold Spring Harbor*; Cold Spring Harbor Laboratory Press: New York, NY, USA, 1999.
6. Boyko, K.M.; Timofeev, V.I.; Samygina, V.R.; Kuranova, I.P.; Popov, V.O.; Koval'chuk, M.V. Protein crystallization under microgravity conditions. Analysis of the results of Russian experiments performed on the international space station in 2005–2015. *Crystallogr. Rep.* **2016**, *61*, 718–729. [[CrossRef](#)]
7. Takahashi, S.; Ohta, K.; Furubayashi, N.; Yan, B.; Koga, M.; Wada, Y.; Yamada, M.; Inaka, K.; Tanaka, H.; Miyoshi, H.; et al. Jaxa protein crystallization in space: Ongoing improvements for growing high-quality crystals. *J. Synchrotron Radiat.* **2013**, *20*, 968–973. [[CrossRef](#)] [[PubMed](#)]
8. Nakano, H.; Hosokawa, A.; Tagawa, R.; Inaka, K.; Ohta, K.; Nakatsu, T.; Kato, H.; Watanabe, K. Crystallization and preliminary x-ray crystallographic analysis of Pz peptidase B from geobacillus collagenovorans MO-1. *Acta Crystallogr. Sect. F Struct. Boil. Cryst. Commun.* **2012**, *68*, 757–759. [[CrossRef](#)] [[PubMed](#)]
9. Inaka, K.; Takahashi, S.; Aritake, K.; Tsurumura, T.; Furubayashi, N.; Yan, B.; Hirota, E.; Sano, S.; Sato, M.; Kobayashi, T.; et al. High-quality protein crystal growth of mouse lipocalin-type prostaglandin d synthase in microgravity. *Cryst. Growth Des.* **2011**, *11*, 2107–2111. [[CrossRef](#)] [[PubMed](#)]
10. DeLucas, L.J.; Moore, K.M.; Long, M.M.; Rouleau, R.; Bray, T.; Crysel, W.; Weise, L. Protein crystal growth in space, past and future. *J. Cryst. Growth* **2002**, *237*, 1646–1650. [[CrossRef](#)]
11. Otalora, F.; Novella, M.L.; Rondon, D.; Garcia-Ruiz, J.M. Growth of lysozyme crystals under microgravity conditions in the Ims (sts-78) mission. *J. Cryst. Growth* **1999**, *196*, 649–664. [[CrossRef](#)]
12. Ng, J.D.; Lorber, B.; Giege, R.; Koszelak, S.; Day, J.; Greenwood, A.; McPherson, A. Comparative analysis of thaumatin crystals grown on earth and in microgravity. *Acta Crystallogr. Sect. D Boil. Crystallogr.* **1997**, *53*, 724–733. [[CrossRef](#)] [[PubMed](#)]
13. McPherson, A. Virus and protein crystal-growth on earth and in microgravity. *J. Phys. D Appl. Phys.* **1993**, *26*, B104–B112. [[CrossRef](#)]
14. Day, J.; McPherson, A. Macromolecular crystal-growth experiments on international microgravity laboratory-1. *Protein Sci.* **1992**, *1*, 1254–1268. [[CrossRef](#)] [[PubMed](#)]
15. DeLucas, L.J.; Smith, C.D.; Smith, H.W.; Vijay-Kumar, S.; Senadhi, S.E.; Ealick, S.E.; Carter, D.C.; Snyder, R.S.; Weber, P.C.; Salemme, F.R.; et al. Protein crystal growth in microgravity. *Science* **1989**, *246*, 651–654. [[CrossRef](#)] [[PubMed](#)]
16. Snell, E.H.; Helliwell, J.R. Macromolecular crystallization in microgravity. *Rep. Prog. Phys.* **2005**, *68*, 799–853. [[CrossRef](#)]
17. Maes, D.; Evrard, C.; Gavira, J.A.; Sleutel, M.; De Weedt, C.V.; Otalora, F.; Garcia-Ruiz, J.M.; Nicolis, G.; Martial, J.; Decanniere, K. Toward a definition of x-ray crystal quality. *Cryst. Growth Des.* **2008**, *8*, 4284–4290. [[CrossRef](#)]
18. Pan, W.; Xu, J.; Tsukamoto, K.; Koizumi, M.; Yamazaki, T.; Zhou, R.; Li, A.; Fu, Y. Crystal growth of hen egg-white lysozyme (hewl) under various gravity conditions. *J. Cryst. Growth* **2013**, *377*, 43–50. [[CrossRef](#)]
19. Niimura, N.; Kurihara, K.; Ataka, M. Dissolution rate of hen egg-white lysozyme crystal under microgravity. *Uchu Seibutsu Kagaku* **2001**, *15*, S176. [[CrossRef](#)] [[PubMed](#)]
20. Kundrot, C.E.; Judge, R.A.; Pusey, M.L.; Snell, E.H. Microgravity and Macromolecular Crystallography. *Cryst. Growth Des.* **2001**, *1*, 87–99. [[CrossRef](#)]
21. Vergara, A.; Lorber, B.; Sauter, C.; Giegé, R.; Zagari, A. Lessons from crystals grown in the Advanced Protein Crystallisation Facility for conventional crystallisation applied to structural biology. *Biophys. Chem.* **2005**, *118*, 102–112. [[CrossRef](#)] [[PubMed](#)]
22. Suzuki, Y.; Tsukamoto, K.; Yoshizaki, I.; Miura, H.; Fujiwara, T. First direct observation of impurity effects on the growth rate of tetragonal lysozyme crystals under microgravity as measured by interferometry. *Cryst. Growth Des.* **2015**, *15*, 4787–4794. [[CrossRef](#)]
23. Yoshizaki, I.; Tsukamoto, K.; Yamazaki, T.; Murayama, K.; Oshi, K.; Fukuyama, S.; Shimaoka, T.; Suzuki, Y.; Tachibana, M. Growth rate measurements of lysozyme crystals under microgravity conditions by laser interferometry. *Rev. Sci. Instrum.* **2013**, *84*, 103707. [[CrossRef](#)] [[PubMed](#)]
24. Judge, R.A.; Snell, E.H.; Woerd, M.J. Extracting trends from two decades of microgravity macromolecular crystallization history. *Acta Crystallogr. Sect. D Boil. Crystallogr.* **2005**, *61*, 763–771. [[CrossRef](#)] [[PubMed](#)]

25. Adawy, A.; van der Heijden, E.G.G.; Hekelaar, J.; van Enckevort, W.J.P.; de Grip, W.J.; Vlieg, E. A comparative study of impurity effects on protein crystallization: Diffusive versus convective crystal growth. *Cryst. Growth Des.* **2015**, *15*, 1150–1159. [[CrossRef](#)]
26. Sleutel, M.; Van Driessche, A.E.S. On the self-purification cascade during crystal growth from solution. *Cryst. Growth Des.* **2013**, *13*, 688–695. [[CrossRef](#)]
27. Weaver, M.L.; Qiu, S.R.; Friddle, R.W.; Casey, W.H.; De Yoreo, J.J. How the overlapping time scales for peptide binding and terrace exposure lead to nonlinear step dynamics during growth of calcium oxalate monohydrate. *Cryst. Growth Des.* **2010**, *10*, 2954–2959. [[CrossRef](#)] [[PubMed](#)]
28. Lee, C.P.; Chernov, A.A. Solutal convection around growing protein crystals and diffusional purification in space. *J. Cryst. Growth* **2002**, *240*, 531–544. [[CrossRef](#)]
29. Vekilov, P.G.; Rosenberger, F.; Lin, H.; Thomas, B.R. Nonlinear dynamics of layer growth and consequences for protein crystal perfection. *J. Cryst. Growth* **1999**, *196*, 261–275. [[CrossRef](#)]
30. Kurihara, K.; Miyashita, S.; Sazaki, G.; Nakada, T.; Durbin, S.D.; Komatsu, H.; Ohba, T.; Ohki, K. Incorporation of impurity to a tetragonal lysozyme crystal. *J. Cryst. Growth* **1999**, *196*, 285–290. [[CrossRef](#)]
31. Vekilov, P.G.; Rosenberger, F. Protein crystal growth under forced solution flow: Experimental setup and general response of lysozyme. *J. Cryst. Growth* **1998**, *186*, 251–261. [[CrossRef](#)]
32. Carter, D.C.; Lim, K.; Ho, J.X.; Wright, B.S.; Twigg, P.D.; Miller, T.Y.; Chapman, J.; Keeling, K.; Ruble, J.; Vekilov, P.G.; et al. Lower dimer impurity incorporation may result in higher perfection of HEWL crystals grown in microgravity A case study. *J. Cryst. Growth* **1999**, *196*, 623–637. [[CrossRef](#)]
33. Snell, E.H.; Judge, R.A.; Crawford, L.; Forsythe, E.L.; Pusey, M.L.; Sportiello, M.; Todd, P.; Bellamy, H.; Lovelace, J.; Cassanto, J.M.; et al. Investigating the effect of impurities on macromolecule crystal growth in microgravity. *Cryst. Growth Des.* **2001**, *1*, 151–158. [[CrossRef](#)]
34. Annunziata, O.; Paduano, L.; Pearlstein, A.J.; Miller, D.G.; Albright, J.G. Extraction of thermodynamic data from ternary diffusion coefficients. Use of precision diffusion measurements for aqueous lysozyme chloride-NaCl at 25 °C to determine the change of lysozyme chloride chemical potential with increasing NaCl concentration well into the supersaturated region. *J. Am. Chem. Soc.* **2000**, *122*, 5916–5928.
35. Pletser, V.; Minster, O.; Bosch, R.; Potthast, L.; Stapelmann, J. The protein crystallisation diagnostics facility: Status of the ESA programme on the fundamentals of protein crystal growth. *J. Cryst. Growth* **2001**, *232*, 439–449. [[CrossRef](#)]
36. Yin, D.-C.; Lu, H.-M.; Geng, L.-Q.; Shi, Z.-H.; Luo, H.-M.; Li, H.-S.; Ye, Y.-J.; Guo, W.-H.; Shang, P.; Wakayama, N.I. Growing and dissolving protein crystals in a levitated and containerless droplet. *J. Cryst. Growth* **2008**, *310*, 1206–1212. [[CrossRef](#)]
37. Yin, D.C.; Oda, Y.; Wakayama, N.I.; Ataka, M. New morphology, symmetry, orientation and perfection of lysozyme crystals grown in a magnetic field when paramagnetic salts (NiCl₂, CoCl₂ and MnCl₂) are used as crystallizing agents. *J. Cryst. Growth* **2003**, *252*, 618–625. [[CrossRef](#)]
38. Sazaki, G.; Yoshida, E.; Komatsu, H.; Nakada, T.; Miyashita, S.; Watanabe, K. Effects of a magnetic field on the nucleation and growth of protein crystals. *J. Cryst. Growth* **1997**, *173*, 231–234. [[CrossRef](#)]
39. Garcia-Ruiz, J.M.; Novella, M.L.; Moreno, R.; Gavira, J.A. Agarose as crystallization media for proteins i: Transport processes. *J. Cryst. Growth* **2001**, *232*, 165–172. [[CrossRef](#)]
40. Van Driessche, A.E.S.; Otalora, F.; Gavira, J.A.; Sazaki, G. Is agarose an impurity or an impurity filter? In situ observation of the joint gel/impurity effect on protein crystal growth kinetics. *Cryst. Growth Des.* **2008**, *8*, 3623–3629. [[CrossRef](#)]
41. Yu, Y.; Wang, X.; Oberthuer, D.; Meyer, A.; Perbandt, M.; Duan, L.; Kang, Q. Design and application of a microfluidic device for protein crystallization using an evaporation-based crystallization technique. *J. Appl. Crystallogr.* **2012**, *45*, 53–60. [[CrossRef](#)]
42. Maeki, M.; Teshima, Y.; Yoshizuka, S.; Yamaguchi, H.; Yamashita, K.; Miyazaki, M. Controlling protein crystal nucleation by droplet-based microfluidics. *Chem. Eur. J.* **2014**, *20*, 1049–1056. [[CrossRef](#)] [[PubMed](#)]
43. Maeki, M.; Yamaguchi, H.; Yamashita, K.; Nakamura, H.; Miyazaki, M.; Maeda, H. A method for generating single crystals that rely on internal fluid dynamics of microdroplets. *Chem. Commun.* **2012**, *48*, 5037–5039. [[CrossRef](#)] [[PubMed](#)]
44. Maeki, M.; Yamazaki, S.; Pawate, A.S.; Ishida, A.; Tani, H.; Yamashita, K.; Sugishima, M.; Watanabe, K.; Tokeshi, M.; Kenis, P.J.A.; et al. A microfluidic-based protein crystallization method in 10 micrometer-sized crystallization space. *CrystEngComm* **2016**, *18*, 7722–7727. [[CrossRef](#)]

45. Leng, J.; Salmon, J.-B. Microfluidic crystallization. *Lab Chip* **2009**, *9*, 24–34. [[CrossRef](#)] [[PubMed](#)]
46. Ng, J.D.; Stevens, R.C.; Kuhn, P. Protein crystallization in restricted geometry: Advancing old ideas for modern times in structural proteomics. *Methods Mol. Biol.* **2008**, *426*, 363–376.
47. Vergara, A.; Lorber, B.; Zagari, A.; Giege, R. Physical aspects of protein crystal growth investigated with the Advanced Protein Crystallization Facility in reduced-gravity environments. *Acta Crystallogr. D Biol. Crystallogr.* **2003**, *59*, 2–15. [[CrossRef](#)] [[PubMed](#)]
48. Maeki, M.; Yamaguchi, H.; Tokeshi, M.; Miyazaki, M. Microfluidic approaches for protein crystal structure analysis. *Anal. Sci.* **2016**, *32*, 3–9. [[CrossRef](#)] [[PubMed](#)]
49. Li, L.; Ismagilov, R.F. Protein crystallization using microfluidic technologies based on valves, droplets and slipchip. In *Annual Review of Biophysics*; Rees, D.C., Dill, K.A., Williamson, J.R., Eds.; Annual Reviews: Palo Alto, CA, USA, 2010; Volume 39, pp. 139–158.
50. Hansen, C.L.; Skordalakes, E.; Berger, J.M.; Quake, S.R. A robust and scalable microfluidic metering method that allows protein crystal growth by free interface diffusion. *Proc. Natl. Acad. Sci. USA* **2002**, *99*, 16531–16536. [[CrossRef](#)] [[PubMed](#)]
51. Hansen, C.L.; Classen, S.; Berger, J.M.; Quake, S.R. A microfluidic device for kinetic optimization of protein crystallization and in situ structure determination. *J. Am. Chem. Soc.* **2006**, *128*, 3142–3143. [[CrossRef](#)] [[PubMed](#)]
52. Zheng, B.; Roach, L.S.; Ismagilov, R.F. Screening of protein crystallization conditions on a microfluidic chip using nanoliter-size droplets. *J. Am. Chem. Soc.* **2003**, *125*, 11170–11171. [[CrossRef](#)] [[PubMed](#)]
53. Yadav, M.K.; Gerdtts, C.J.; Sanishvili, R.; Smith, W.W.; Roach, L.S.; Ismagilov, R.F.; Kuhn, P.; Stevens, R.C. In situ data collection and structure refinement from microcapillary protein crystallization. *J. Appl. Crystallogr.* **2005**, *38*, 900–905. [[CrossRef](#)] [[PubMed](#)]
54. Zheng, B.; Gerdtts, C.J.; Ismagilov, R.F. Using nanoliter plugs in microfluidics to facilitate and understand protein crystallization. *Curr. Opin. Struct. Biol.* **2005**, *15*, 548–555. [[CrossRef](#)] [[PubMed](#)]
55. Shim, J.-U.; Cristobal, G.; Link, D.R.; Thorsen, T.; Fraden, S. Using microfluidics to decouple nucleation and growth of protein crystals. *Cryst. Growth Des.* **2007**, *7*, 2192–2194. [[CrossRef](#)] [[PubMed](#)]
56. Shim, J.-U.; Cristobal, G.; Link, D.R.; Thorsen, T.; Jia, Y.; Piattelli, K.; Fraden, S. Control and measurement of the phase behavior of aqueous solutions using microfluidics. *J. Am. Chem. Soc.* **2007**, *129*, 8825–8835. [[CrossRef](#)] [[PubMed](#)]
57. Sauter, C.; Dhoub, K.; Lorber, B. From macrofluidics to microfluidics for the crystallization of biological macromolecules. *Cryst. Growth Des.* **2007**, *7*, 2247–2250. [[CrossRef](#)]
58. Carruthers, C.W., Jr.; Gerdtts, C.; Johnson, M.D.; Webb, P. A microfluidic, high throughput protein crystal growth method for microgravity. *PLoS ONE* **2013**, *8*. [[CrossRef](#)] [[PubMed](#)]
59. Paxton, T.E.; Sambanis, A.; Rousseau, R.W. Influence of vessel surfaces on the nucleation of protein crystals. *Langmuir* **2001**, *17*, 3076–3079. [[CrossRef](#)]
60. Garcia-Ruiz, J.M.; Gonzalez-Ramirez, L.A.; Gavira, J.A.; Otálora, F. Granada Crystallisation Box: A new device for protein crystallisation by counter-diffusion techniques. *Acta Crystallogr. D Biol. Crystallogr.* **2002**, *58*, 1638–1642. [[CrossRef](#)] [[PubMed](#)]
61. Meirong, L.; Nadarajah, A.; Pusey, M.L. Growth of (101) faces of tetragonal lysozyme crystals: Determination of the growth mechanism. *Acta Crystallogr. D Biol. Crystallogr.* **1999**, *55*, 1012–1022.
62. Nadarajah, A.; Pusey, M.L. Growth mechanism and morphology of tetragonal lysozyme crystals. *Acta Crystallogr. Sect. D Biol. Crystallogr.* **1996**, *52*, 983–996. [[CrossRef](#)] [[PubMed](#)]
63. Ferreira, C.; Barbosa, S.; Taboada, P.; Rocha, F.A.; Damas, A.M.; Martins, P.M. The nucleation of protein crystals as a race against time with on- and off-pathways. *J. Appl. Cryst.* **2017**, *50*, 1056–1065. [[CrossRef](#)]
64. Nadarajah, A.; Meirong, L.; Pusey, M.L. Growth mechanism of the (110) face of tetragonal lysozyme crystals. *Acta Crystallogr. D Biol. Crystallogr.* **1997**, *53*, 524–534. [[CrossRef](#)] [[PubMed](#)]
65. Kadowaki, A.; Yoshizaki, L.; Rong, L.; Komatsu, H.; Odawara, O.; Yoda, S. Improvement of protein crystal quality by forced flow solution. *J. Synchrotron Radiat.* **2004**, *11*, 38–40. [[CrossRef](#)] [[PubMed](#)]

